Phase transitions in electrorheological fluids using molecular dynamics simulations

Giovanni Lapenta,[1,2,*] Giovanni Maizza,[1,3] Antonio Palmieri[3], Gianmarco Boretto,[4] and Massimo Debenedetti[4]
[1]*Istituto Nazionale per la Fisica della Materia, Unità del Politecnico di Torino, Torino, Italy*
[2]*Dipartimento di Energetica, Politecnico di Torino, Corso Duca degli Abruzzi 24, Torino, Italy*
[3]*Dipartimento di Scienza dei Materiali e Ingegneria Chimica, Politecnico di Torino, Torino, Italy*
[4]*Centro Ricerche FIAT, Orbassano, Italy*
(Received 28 April 1999)

A parametric study of the properties of electrorheological fluids is conducted using molecular dynamics (MD) simulations. The MD model is based on the solution of the Langevin equation for a number of suspended particles. The equations of motion include inertial effects, polarization forces, Stokes' drag, short range repulsion, and Brownian forces. Different polarization forces are considered to include the effect of enhancements at short range due to multipole moments induced by the suspended particles and other effects. The model is used to investigate the structural changes induced by external electric fields and by shear strains imposed on the system. The response times are studied as a function of two characteristic parameters describing the physical status of the system (temperature and external electric field). Finally, the stress-strain characteristics are studied and the yield stress is calculated as a function of the external electric field. The simulated response is compared with experimental findings. [S1063-651X(99)14710-X]

PACS number(s): 83.20.Jp, 83.80.Gv, 83.50.Nj

I. INTRODUCTION

Electrorheological (ER) fluids are a class of materials that undergo a liquid to solid transition under the effect of an external electric field. After their discovery [1], several applications of ER fluids have been proposed in various fields of automotive and aerospace engineering, structural engineering, and many others [2]. The interest in ER materials continues today as new improved fluids are proposed and new applications are considered. However, at present the commercial use of ER devices is still limited. The properties of ER fluids need further improvement before commercial applications become more widely available. More studies are needed to understand fully the ER process and to design new ER fluids with properties suitable for practical applications.

In the present work, we study the simulation models most commonly used in ER research. We use a molecular dynamics model based on interaction potentials presented in the literature [3,4]. The performance of the model is assessed with a parametric study of the properties of the simulated fluid. The study uses two dimensionless parameters related to the temperature of the system and to the externally applied electric field. The effect of the two parameters is studied for three aspects.

First, we evaluate the structural changes in a ER fluid and the effect of the two control parameters. The effect on the structure of an ER fluid due to shear strains imposed on the system is also considered.

Second, the response times of an ER fluid is studied as a function of the two control parameters. The effect of thermal motions and of the relative strength of the polarization forces is considered. Different polarization forces proposed in the literature are implemented and their effect on the response times is studied.

Third, the rheological properties of the simulated systems are obtained. The stress-strain characteristic is derived from the results of several simulations.

To investigate the reliability of simulation studies, the simulation results are compared with previous experimental findings when possible.

The present paper is organized as follows. Section II describes in detail the molecular dynamics model used in the present work and the diagnostics used to extract information on the evolution of the system. Section III describes the structural changes in an ER fluid under the effect of external electric fields and shear strains. Section IV reports a parametric study of the response times of ER fluids for various choices of the control parameters. Section V reports the rheological properties of the simulated systems. The Conclusions section summarizes the results and points to future developments needed to improve the accuracy of simulation studies.

II. SIMULATION MODEL

The simulation model is based on the molecular dynamics (MD) method [5]. A small portion of the system is considered and periodic boundary conditions are applied on all boundaries. The computational domain includes a given number (ranging from 50 to 100 in the simulations described below) of spherical dielectric particles with diameter a immersed in a fluid matrix. We follow an approach similar to previous works [3] and based on the Langevin equation of motion for each particle p:

$$m\frac{d^2\mathbf{x}_p}{dt^2}=\sum_{p'}\frac{\partial\Phi_{pp'}}{\partial\mathbf{x}_p}-3\pi a\eta\frac{d\mathbf{x}_p}{dt}+\mathbf{R}_p, \tag{1}$$

where the interaction potential $\Phi_{pp'}$ includes all interactions between the particles, $3\pi a\eta(d\mathbf{x}_p/dt)$ is the Stokes drag force, and $\mathbf{R}_p$ is the Brownian force.

*Electronic address: lapenta@polito.it

 © 1999 The American Physical Society

The most important aspect of the MD model is the choice of the interaction potential $\Phi_{pp'}$. In the present work, the potential includes a long-range potential arising from the polarization of the suspended particles and a short-range repulsion responsible for the integrity of the suspended particles.

The long-range interaction potential is due to the polarization of the suspended particles induced by electric fields applied externally. In its simplest form, the interaction is due to a dipole-dipole potential. It is assumed that all particles are spheres with diameter a and the same dipole moment is induced on all particles:

$$\mu = \frac{1}{2}\frac{\epsilon_f(\epsilon_p - \epsilon_f)}{2\epsilon_f + \epsilon_p} a^3 E, \tag{2}$$

where $\epsilon_f(\epsilon_p)$ is the dielectric constant of the fluid matrix (dispersed particles). The external electric field E and the dipole moment μ are assumed parallel to the vertical axis z. In this approximation the dipole interaction potential is

$$\Phi_{D,pp'} = -\frac{\mu^2}{4\pi\epsilon_f r_{pp'}^3}(3\cos^2\theta_{pp'} - 1), \tag{3}$$

where $r_{pp'}(\theta_{pp'})$ is the distance (angle with respect to axis z) between particle p and p'.

Expression (3) neglects the additional multipoles induced by one suspended particle on another at close range. This effect has been shown to enhance very significantly the ER effect [6]. A simple improvement to Eq. (3) is achieved using the enhanced interaction potential proposed by Whittle [4]:

$$\Phi_{W,pp'} = \Phi_{D,pp'}(1 + \lambda e^{-(r_{pp'} - a)/r_0}). \tag{4}$$

The parameters r_0 and λ can be chosen to represent different interaction processes [4]. When $\lambda = 0$, the potential becomes simply the dipole-dipole interaction potential. We considered also the choice $r_0 = 0.1$ and $\lambda = 5$, suggested by Whittle [4], that leads to an enhancement of the interaction force only at short ranges (i.e., at distances of the order of $r_0 a$).

The interaction potential includes a short-range repulsion component

$$\Phi_{R,pp'} = \frac{3\mu^2 L_R}{2\pi\epsilon_f a^3}\left(1 + \lambda + \frac{a\lambda}{3r_0}\right) e^{-(r_{pp'}/a - 1)/L_R}. \tag{5}$$

The amplitude of the repulsion potential is chosen in order to give a net zero force when two particles are in contact. The interaction length of the short-range repulsion potential must be small enough to ensure the dominance of the dipole interaction when two particles are not in contact. A value $L_R = 1/13$ is used. The Brownian force is implemented using a Nosé-Hoover thermostat, as is common in MD simulations [5]: the Brownian force is obtained sampling a normal distribution with variance Λ_B.

The model equations (1) are advanced in time using the interaction potentials given above. The simulation starts from initial disorder (the particles are initially distributed randomly) and is continued long enough to investigate the dynamics of the liquid to solid phase transition induced by an external electric field. The evolution of the system is studied monitoring the positions of all particles. The simulations can also include a prescribed velocity field applied to the simulation box: at the end of each computational cycle, all particle positions are shifted according to a specified velocity field [7]. The prescribed strain is used to measure the stress-strain characteristics of ER fluids.

Different transport parameters are calculated during the simulation, including the diffusion tensor

$$D_{\alpha\beta} = \frac{1}{2t}\sum_p [x_{\alpha p}(t) - x_{\alpha p}(0)][x_{\beta p}(t) - x_{\beta p}(0)], \tag{6}$$

the mean distance traveled by a particle along coordinate α:

$$d_{\alpha\alpha} = (2tD_{\alpha\alpha})^{1/2} \tag{7}$$

and the stress tensor

$$\tau_{\alpha\beta} = \frac{1}{2V}\sum_p \sum_{p' \neq p} \frac{(x_{\alpha p} - x_{\alpha p'})(x_{\beta p} - x_{\beta p'})}{r_{pp'}} \mathbf{F}_{pp'}. \tag{8}$$

In Eqs. (6)–(8), α, β label the coordinates, V is the volume of the system, and $\mathbf{F}_{pp'}$ is the interaction force.

The computer simulations and the results described below are expressed in normalized units [3]. The normalized time is $\varsigma = t(3\pi a\eta)/m$, the normalized length scale is $\vec{\xi} = \mathbf{x}/a$, and the normalized force is $\vec{\mathcal{F}} = \mathbf{F}4\pi\epsilon_f a^4/3p^2$. All other derived quantities (e.g., $D_{\alpha\beta}$, $d_{\alpha\alpha}, \tau_{\alpha\beta}$) are normalized accordingly.

Two dimensionless parameters can be introduced to categorize the simulations:

$$A = \frac{\mathrm{Re}}{\mathrm{Mn}},$$

$$B = \frac{\Lambda_B a^4 \epsilon_f}{3\mu^2}. \tag{9}$$

Parameter A is the ratio of the Reynold number $\mathrm{Re} = mv/3\pi\eta a^2$ and the Mason number $\mathrm{Mn} = 4\pi^2\epsilon_f a^5 \eta v/\mu^2$ and represents the strength of the interaction induced by the polarization of the particles. Parameter B is the ratio of the Brownian force and of the dipole force. Note that many different fluids can have the same values of A and B; thus every simulation represents an entire class of fluids.

III. STRUCTURE OF ER FLUIDS UNDER STRESS

The typical evolution of the system from an initial disordered state leads to the formation of chains of particles aligned along the external electric field. The final structure is affected largely by the relative strength of the polarization effect, the Stokes drag of the fluid matrix and the Brownian force. Previous studies [3] have shown that for large B and/or small A the final structure remains chaotic. Only for sufficiently small values of B (small thermal fluctuations) and large values of A (strong polarization) is the ER effect present, and the system undergoes a phase transition where the final state is characterized by chains of particles aligned along the z axis.

In the present work, we consider also the effect of strains

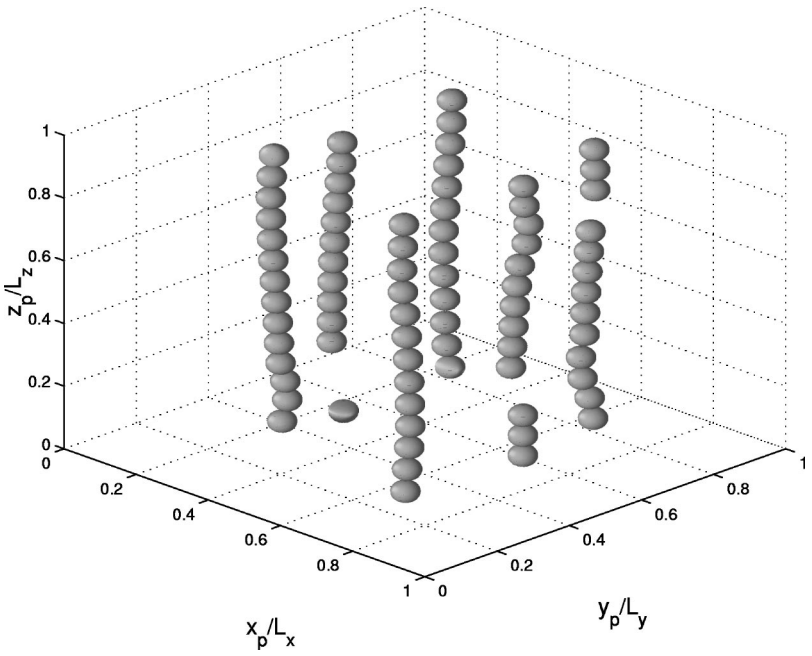

FIG. 1. Positions of 78 particles at the end ($\varsigma = 80$) of a simulation with $A = 0.5$, $B = 0.01$, $\lambda = 0$, $\dot{\gamma} = 0$, and volume fraction 12%.

imposed externally, to simulate ER fluids under stress. In this case, a constant shear strain is imposed along the x direction, corresponding to a velocity field linearly varying along the vertical direction ($\mathbf{v} = \hat{\mathbf{x}}\dot{\gamma}z$). As the shear strain rate $\dot{\gamma}$ is increased, the chains formed by the suspended particles tend to bend in the direction of the flow, creating an internal stress opposed to the external action. As the shear strain rate is increased beyond a critical value, the chains break and the system returns to a disordered state.

Figures 1 and 2 make a comparison between a typical chain structure in the absence of external strain (Fig. 1) and an external strain rate $\dot{\gamma} = 0.15$ (Fig. 2). The results are relative to the case $A = 0.5$ and $B = 0.01$ at time $\varsigma = 80$. The system undergoes a phase transition in both cases. In the absence of imposed strains, at the end of the simulation the particles are aligned along the vertical direction; in the presence of strain, the chains are inclined in the direction of strain. The strained state is characterized by a stress tensor in response to the external action (see Sec. V). Similar behavior is observed for other parameters A, B.

IV. RESPONSE TIMES

A critical feature of the ER response is the time required to reach the final ordered state. Figure 3 shows the typical evolution of the diffusion coefficient observed in the simulations. The system is characterized by two time scales: the diffusion coefficient increases initially very rapidly (note the logarithmic scale in Fig. 3), reaches a peak value, and then decreases much more slowly. This behavior can be understood observing the evolution of the positions of all the particles in the system. The initial rapid response corresponds to

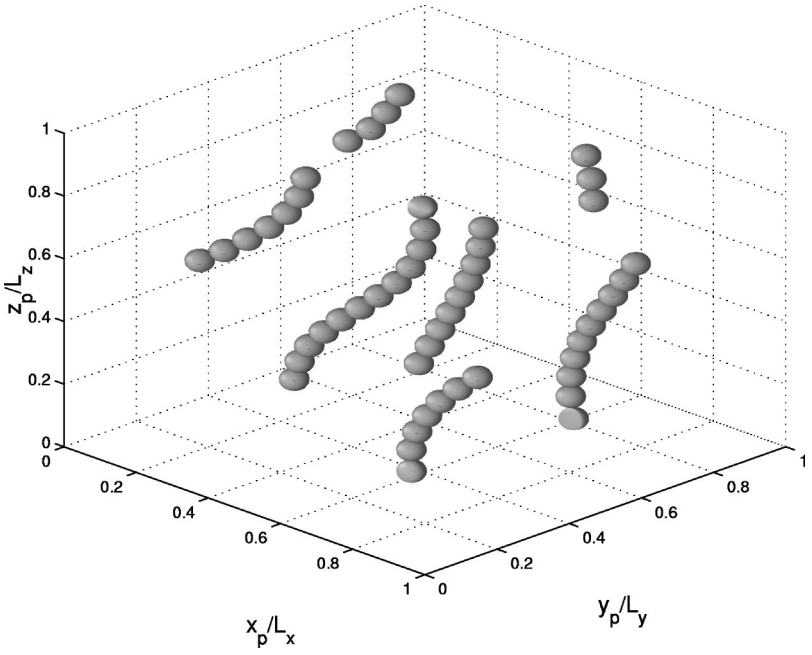

FIG. 2. Positions of 52 particles at the end ($\varsigma = 80$) of a simulation with $A = 0.5$, $B = 0.01$, $\lambda = 0$, $\dot{\gamma} = 0.15$, and volume fraction 12%.

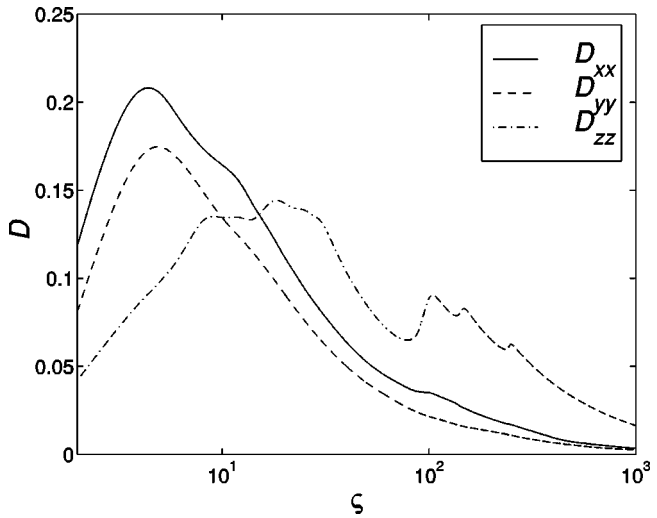

FIG. 3. Evolution of the diffusion coefficient $D_{\alpha\alpha}$, in dimensionless units. Simulation with $A=0.5$, $B=0.01$, $\lambda=0$, $\dot{\gamma}=0$, and volume fraction 12%.

the process of chain formation. The particles start from a random disorder and quickly pack in a few chains. Once the process of chain formation is completed, the diffusion coefficient reaches its peak value and starts to decrease much more slowly. This latter process corresponds to an adjustment of the structure of the chains already formed. At the end of the initial fast process of chain formation, the chains have particles displaced from their perfectly aligned position. The slow adjustments of the second phase lead to a more ordered structure where the final configuration is characterized by almost perfect columns of particles.

At the time when the chains are first formed (corresponding to the peak time in Fig. 3), ER fluids start to present a yield stress. As a consequence, the ER response time, defined as the time when the yield stress becomes active, can be identified as the time corresponding to the peak of the diffusion coefficient [4]. However, the slower adjustments following the time when the peak is reached are also relevant, as the yield stress can increase significantly as the chains adjust and increase their order. Another important response time is the mean time required for two particles to come into contact, i.e., the mean time needed to travel the average distance between the particles.

TABLE I. Normalized times required for the diffusion coefficient to reach its peak value; case with $\lambda=0$ (dipole interaction).

A	B	$\varsigma_{p\perp}$	$\varsigma_{p\parallel}$
0.005	0.05	715	1810
0.005	0.1	700	2800
0.005	0.5	810	390
0.005	1	380	2380
0.05	0.05	39	175
0.05	0.1	40	180
0.05	0.5	60	60
0.05	1	38	135
0.5	0.05	5	8
0.5	0.1	9	25
0.5	0.5	4	16
0.5	1	4	16

TABLE II. Normalized times required for the diffusion coefficient to reach its peak value; case with $\lambda=5$, $r_0=0.1$ (enhanced interaction).

A	B	$\varsigma_{p\perp}$	$\varsigma_{p\parallel}$
0.5	0	5	8
0.5	0.01	5	8
0.5	0.05	4	8
0.5	0.1	5	9
0.5	0.5	5	22
0.5	1	5	19

The response times have been measured in several simulations. In all cases four times are calculated: the peak time and the contact time in the z direction parallel to the applied field $\varsigma_{p\parallel}, \varsigma_{c\parallel}$ and the peak time and the contact time in the plane perpendicular to the applied field $\varsigma_{p\perp}, \varsigma_{c\perp}$ (measured as the average of the times in the x and y directions). In all simulations, the volume fraction is 12%.

Table I shows the peak time for the case of a purely dipole interaction ($\lambda=0$). Table II shows similar results for the case of the enhanced interaction ($\lambda=5$, $r_0=0.1$). Tables III and IV show the contact time for the same cases.

The response times decrease very rapidly as parameter A is increased. Recalling that A measures the polarization force, it means that the response times are reduced as the external field is increased, or as the strength of the ER response is increased. The effect of parameter B on the response times is small; a change of B of one order of magnitude causes changes smaller than a factor of 2.

Comparing Table I with Table II and Table III with Table IV, the effect of changing the expression for the polarization force is small: in general, the enhanced force reduces the response times only marginally. The enhanced force becomes significantly stronger than the dipole-dipole force only once the particles are in close contact, i.e., when the chains are already formed. The response times do not depend significantly on the short-range enhancement. Note that this

TABLE III. Normalized contact times; case with $\lambda=0$ (dipole interaction). In some cases the contact time exceeds the total simulation time (*).

A	B	$\varsigma_{c\perp}$	$\varsigma_{c\parallel}$
0.005	0.05	1535	1870
0.005	0.1	*	210
0.005	0.5	3400	1800
0.005	1	5150	1800
0.05	0.05	*	270
0.05	0.1	865	180
0.05	0.5	*	280
0.05	1	102	280
0.5	0.05	42	24
0.5	0.1	38	19
0.5	0.5	38	16
0.5	1	13	14

TABLE IV. Normalized contact times; case with $\lambda=5, r_0=0.1$ (enhanced interaction).

A	B	$\varsigma_{c\perp}$	$\varsigma_{c\parallel}$
0.5	0	80	12
0.5	0.01	80	12
0.5	0.05	79	14
0.5	0.1	78	12
0.5	0.5	79	14
0.5	1	28	12

conclusion is valid for the specific enhanced interaction used in the present work [Eq. (4)]; if more complete multipolar interactions are used [6], it is possible that more significant changes in the response times can be observed. Moreover, in the present study, the volume fraction of the dispersed particles is kept constant; it is possible that the effect of the short-range enhancement of the polarization force might become more significant if the volume fraction of the dispersed particles were increased and the particles were more closely packed.

The difference between the peak time and the contact time for the same simulation is especially relevant for the case where the enhanced force is used (Tables II and IV). In the parallel direction, the contact time $\varsigma_{c\parallel}$ is similar to the peak time $\varsigma_{\parallel}$, but in the transverse plane, the two times differs significantly. All peak times and the contact time in the parallel direction measure the fast time scale for the chain formation. On the contrary, the contact time in the transverse plane measures the longer time scale for the consolidation of the structure. The different behavior of the response times in the different directions reflects the anisotropy of the motion induced by the external field directed along the z axis.

The response times reported in Tables I–IV, are in normalized units and each case with a given A and B is relative to a class of ER fluids with the same normalized values. For example, the results of the same simulation with $A=0.005, B=0.05$ and with the enhanced interaction (see Table II) can be used to predict the response times of different ER fluids characterized by different sizes of dispersed particles. Figure 4 shows the response time (in ms) as a function of the particle diameter a, for a fluid with viscosity $\eta=35$ mPa s, density of material of the suspended particles 2 g/cm^3, and $\epsilon_p/\epsilon_f=10$. As explained in the Conclusions section below, parameter A is chosen large enough to avoid excessive computational costs. Smaller values of A would be required to make a complete quantitative comparison with experiments. Nevertheless, the response times shown in Fig. 4 are on the same order of magnitude as the experiments.

V. RHEOLOGICAL PROPERTIES

The stress-strain characteristic of an ER fluid is simulated imposing external strains as described in Sec. II. A uniform velocity field is superimposed onto the intrinsic velocity field of the simulation. The system reacts to the external perturbation creating a stress field. In the results reported below, the shear stress is measured using Eq. (8), thereby excluding the contribution of the viscosity of the suspending fluid; to obtain the total shear stress, the effect of the viscosity of the suspending fluid needs to be included [7].

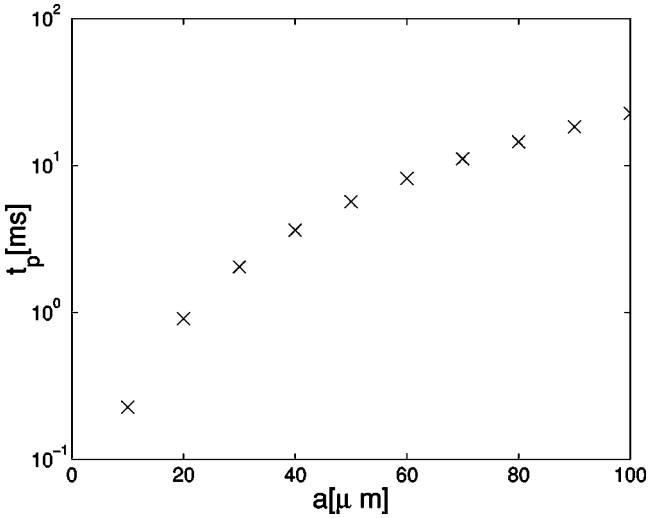

FIG. 4. Response times of a real ER fluid with $\eta=35$ mPa s, $\epsilon_p/\epsilon_f=10$. Data obtained from the simulation results with $A=0.005$, $B=0.05$.

Figure 5 shows the stress-strain characteristic for a system with $A=0.5$ and $B=0.01$, using the enhanced polarization force. The measured shear stress is plotted as a function of the imposed shear strain rate $\partial v_x/\partial z=\dot{\gamma}$. The shear strain is imposed in the x direction; the corresponding shear stress is τ_{xz}. Figure 5 is qualitatively similar to experimental results [2]. The yield stress can be obtained from Fig. 5, extrapolating the curve to $\dot{\gamma}=0$. The analysis is conducted for different values of A (but using in all cases the enhanced polarization force), and the corresponding values of the yield stresses are shown in Fig. 6. The quadratic behavior is the same as that observed in experiments.

A quantitative comparison with experiments can be carried out using typical values for the physical parameters of the ER fluids (viscosity $\eta=0.9$ Pa s, suspended particle radius 100 μm, and dielectric constants $\epsilon_f=2$ and $\epsilon_p=8$). Table V shows the same data as Fig. 6 but in SI (Système

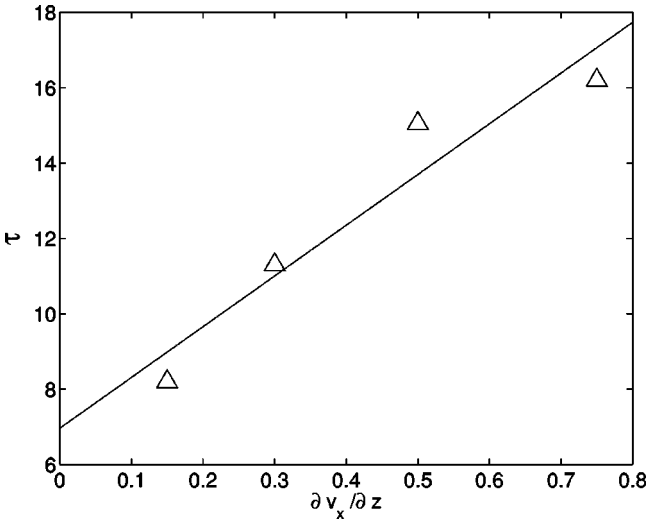

FIG. 5. Stress-strain characteristic in dimensionless units. Simulations with $A=0.5$, $B=0.01$, $\lambda=5$, $r_0=0.1$, and volume fraction 12%.

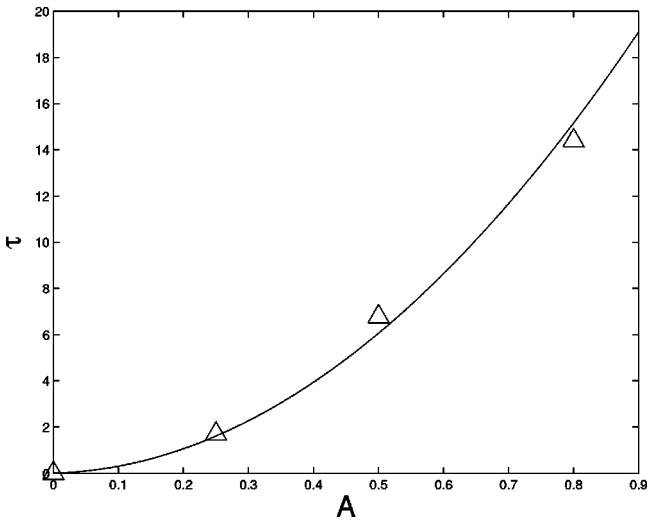

FIG. 6. Bingham yield stress as a function of *A*, in dimensionless units. Simulation with $B=0.01$, $\lambda=5$, $r_0=0.1$, and volume fraction 12%.

Internationale) units rather than in normalized units. Note that Fig. 6 is a general result for a class of similar ER fluids, while the data in Table V are for a specific case only. The simulated results are of the same order of magnitude as actual experimental results.

VI. CONCLUSIONS

A simulation model of ER fluids has been presented. The model is based on the MD approach and includes polarization forces, Brownian forces, Stoke's drag, and short-range repulsion. Different polarization forces have been considered to investigate the effect of enhanced interactions at close range.

TABLE V. Yield stress τ_0 as a function of the external electric field *E*, obtained from the simulation results in Fig. 6 using physical properties of an actual ER fluid.

E (kV/mm)	τ_0 (Pascal)
10.8	30
15.2	145
17.3	310
20	570

Simulations have been run to study the response times and the rheological properties of ER fluids. The results are presented in normalized units, to represent classes of similar fluids. Two dimensionless parameters have been used to categorize the simulations. When possible, comparisons with real ER fluids have been provided.

The results show good qualitative agreement with experimental results. However, further studies to relate the enhanced polarization force with real processes are needed in order to simulate real ER fluids reliably. An improvement in this direction is to use the exact interaction potential that includes the multipoles induced by one suspended particle on another [6].

Furthermore, the present simulations have been confined to parameter ranges that are in part beyond the realistic range. Indeed, for real ER fluids, the parameter *B*, describing the relative strengths of the Brownian forces, lies in the range 10^{-4}–10, well covered in the present study. Instead, the parameter *A*, describing the relative strengths of polarization forces, lies in the range 10^{-6}–10^{-2}, typically smaller than the values used in the present work ($10^{-2}<A<1$). The values of parameter *A* used in the simulations are limited by technical problems with the solution of the Langevin equation, which becomes prohibitively computing intensive at very small values of $A<10^{-2}$.

[1] W.M. Winslow, J. Appl. Phys. **20**, 113 (1949).
[2] U.S. Department of Energy, Office of Energy Research, Report No. DOE/ER/30172 (1993).
[3] G.L. Gulley and R. Tao, Phys. Rev. E **56**, 4328 (1997).
[4] M. Whittle, J. Non-Newtonian Fluid Mech. **37**, 233 (1990).
[5] D. Frenkel and B. Smit, *Understanding Molecular Simulation: From Algorithms to Applications* (Academic Press, San Diego, 1996).
[6] L. Fu and L. Resca, Phys. Rev. B **53**, 2195 (1996).
[7] M. P. Allen and D. J. Tildesley, *Computer Simulation of Liquids* (Clarendon, Oxford, 1987).